# APPARATUS FOR STUDYING
# BALL SPINNING FRICTION

*by Steven T. Miller, Richard J. Parker,*
*and Erwin V. Zaretsky*

*Lewis Research Center*
*Cleveland, Ohio*

# APPARATUS FOR STUDYING BALL SPINNING FRICTION

## By Steven T. Miller, Richard J. Parker, and Erwin V. Zaretsky

### Lewis Research Center
### Cleveland, Ohio

## NATIONAL AERONAUTICS AND SPACE ADMINISTRATION

# APPARATUS FOR STUDYING BALL SPINNING FRICTION

by Steven T. Miller, Richard J. Parker, and Erwin V. Zaretsky

Lewis Research Center

## SUMMARY

2 3 8 1 9

An experimental apparatus was designed and constructed at the NASA Lewis Research Center to study one aspect of spinning friction based on interfacial slip over the entire ball-race contact area. The apparatus is capable of measuring spinning moments of less than 0.01 inch-pound at maximum Hertz contact stresses to over 400 000 psi, speeds to 3500 rpm, and under varying contact configurations and conditions. From the torque measurement, a coefficient of spinning friction can be calculated.

The apparatus comprises a drive assembly, a dead-weight load assembly, a spherical upper test specimen, a cylindrically grooved lower test specimen of varying conformity, a lower test specimen housing assembly incorporating a hydrostatic air-bearing assembly, and a torque-measuring system. In operation, the upper test specimen is loaded against the lower test specimen through the drive shaft assembly by the dead-weight load assembly. As the drive assembly is rotated, the upper test specimen rotates against the stationary lower test specimen actuating the torque-measuring system.

Preliminary tests were conducted under varying Hertz stress to 136 000-psi maximum Hertz stress at a spinning speed of 950 rpm, with a 51 percent ball-groove conformity using a polyphenyl ether (5P4E), a highly purified naphthenic mineral oil, and a di-2-ethylhexyl sebacate (MIL-7808). It was found that the coefficient of spinning friction decreased with increasing maximum Hertz stress to an intermediate stress level and had a minimum value of 0.122, 0.089, and 0.050, respectively, for the lubricants listed previously.

*AuTHOR*

## INTRODUCTION

Space applications having limited power capabilities, such as satellites and manned space vehicles, dictate not only a high degree of system reliability but also an increase in the operating efficiency of the system. Efficiency can be increased by decreasing both weight and frictional losses in payload components. Since rolling-element bearings
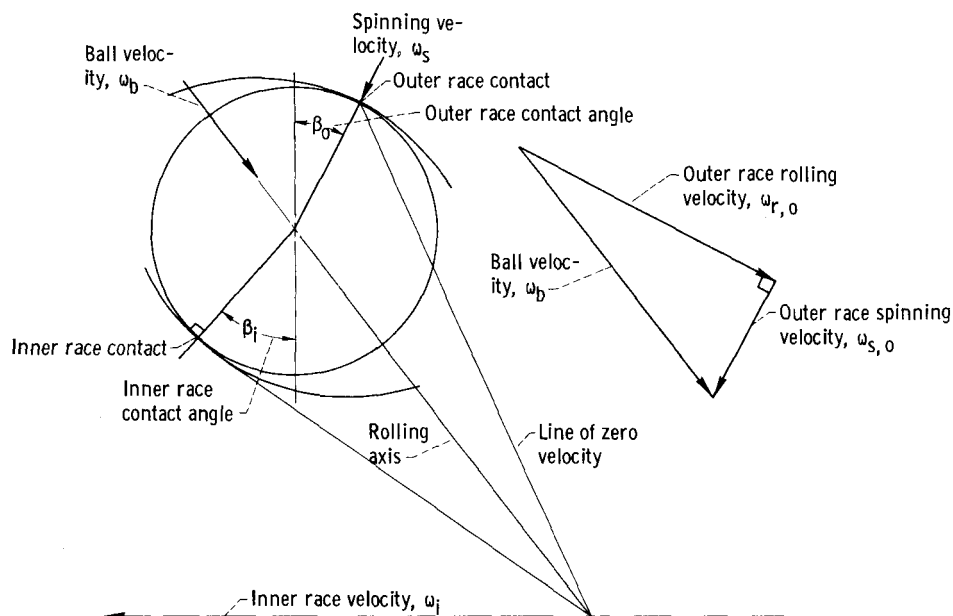
Figure 1. - Bearing geometric relations used to calculate ball spin and inner-race control.

are components of most guidance and space power generating systems, the attainment of highest efficiencies makes it necessary to study closely factors such as bearing kinematics, contact stresses, material deformation, and coefficients of sliding friction that effect bearing power loss (ref. 1).

A significant portion of total ball-bearing friction results from friction due to spinning. For thrust-loaded angular-contact ball bearings, the ball spins about an axis perpendicular to the contact area on either the inner or the outer race depending on ball control (ref. 2). This component, called spinning, is vectorially illustrated by $\omega_s$ in figure 1 for inner race control. Ball control is the ability of either race to impose rolling without spinning on the balls as the bearing rotates about its axis. For ball bearings, ball control is a function of the relative size of the ball-race contact areas, the eccentricity of the contact ellipses, and the coefficient of friction in the contact areas.

Ball spinning motion causes a spinning moment or torque about an axis normal to the contact area. The friction force associated with this moment results from Coulomb friction (see BACKGROUND Section) and/or fluid shear forces, depending on whether dry surface, boundary, or elastohydrodynamic lubrication occurs at the contact interface. The resulting torque contributes to internal bearing losses.

Experimental results reported in references 3 and 4 indicate that interfacial slip may not occur in nonlubricated ball-race contacts over the entire contact area during spinning with rolling. An apparent elastic compliance may occur over a portion of the contact area together with interfacial slip over the remaining portion. The amount of interfacial slip would affect the magnitude of the energy loss in the contact area. Knowledge of the coefficients of friction under pure spinning conditions is necessary for later

2

experiments to determine under what conditions of rolling and spinning elastic compliance occurs. In order to accomplish this, the coefficient of spinning friction must be determined under contact conditions, that is, ball-race conformity, contact stresses, lubricants, and spinning speeds found in conventional ball bearings. Therefore, it was necessary to design and construct a test apparatus that can, as closely as possible, segregate spinning friction losses from other losses found in a bearing. This test apparatus would have to measure accurately spinning torques as low as 0.01 inch-pound (ref. 5).

A test apparatus was designed and built at the NASA Lewis Research Center to study one aspect of spinning friction based on interfacial slip over the entire contact area. An engineering description of the apparatus and preliminary spin friction measurements are presented herein.

# BACKGROUND

Methods for calculating the shape, size, and pressure distribution of the contact areas of two solid, elastic bodies have been derived mathematically by Hertz and are presented in reference 1. The contact area geometry, because of elastic deformation, is elliptical in a ball bearing. The kinematics of component motion within a ball bearing has been studied analytically in references 2 and 6. Because of bearing geometry and associated kinematics, the ball has an angular velocity, called spinning, about an axis perpendicular to the contact area of a ball on either race, depending upon ball control (ref. 2). For inner-race ball control, this component is vectorially illustrated in figure 1.

It was reported in reference 3 that, when a ball rolls with spinning on a plane, interfacial slip due to spinning may not occur over the entire contact area. Rather, under certain conditions of rolling with spinning, a region of no slip may exist near the leading edge of the contact area with an area of slip towards the rear of the contact area. If tangential friction forces are sufficiently great, they may prevent interfacial slip; and, if this occurs, a condition of elastic compliance is said to exist. An analytical study of elastic compliance can be found in reference 7. It was assumed in reference 3 that, for elastic compliance, the bodies in contact are perfectly smooth and hydrodynamic lubrication effects are not present because of the low speeds involved. Therefore, tangential tractions are based on Coulomb-type friction. (Coulomb friction is defined such that friction force is proportional to normal load and independent of the area in contact. Thus, the coefficient of friction is assumed constant over the contact area. Where the sliding velocities are low, Coulomb friction is also independent of velocity.)

The predominant friction phenomenon depends on the contact geometry, the spinning speed, contact stress, and lubricant rheology. Contributions to spin friction would re-
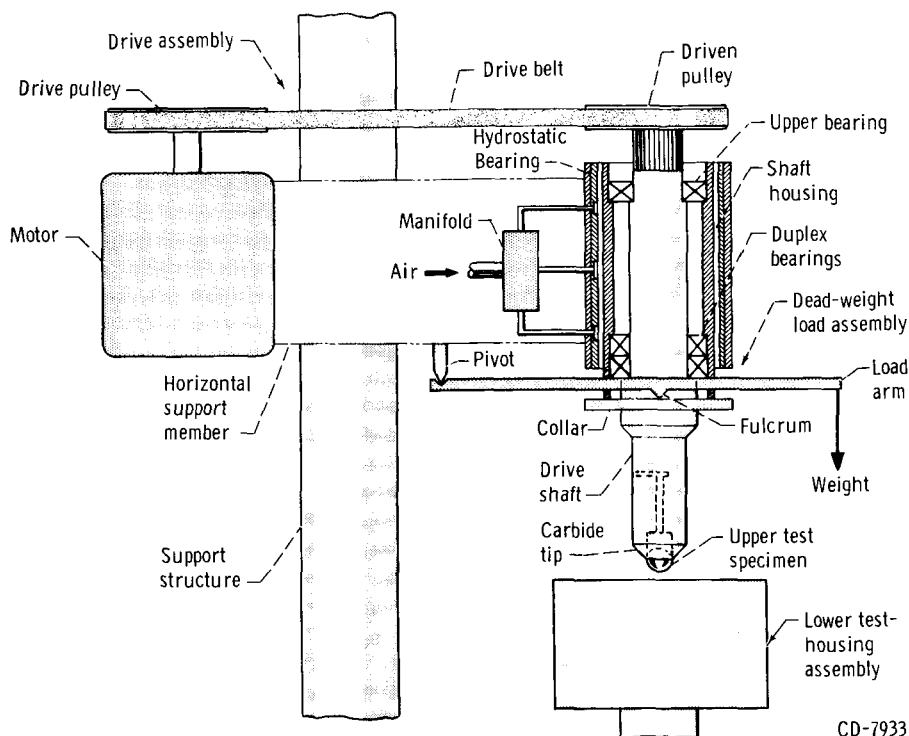
Figure 2. - Spinning-friction apparatus drive and load assemblies.

sult from shearing of an elastohydrodynamic film, Coulomb friction (where there is only a partial film and asperity contact between the rolling elements), and hysteresis losses (where there is complete elastic compliance). It is speculated that both Coulomb and shear friction would be present in the spinning-friction apparatus.

## SPINNING-FRICTION APPARATUS

The spinning-friction apparatus (see figs. 2 and 3) essentially consists of a drive assembly, dead-weight load assembly, an upper and lower test specimen, a lower test-housing assembly incorporating a hydrostatic air-bearing assembly, and a torque-measuring system. In operation, the upper test specimen is loaded against the lower test specimen through the drive-shaft assembly by the dead-weight load assembly. As the drive assembly is rotated, the upper test specimen runs against the stationary lower test specimen actuating the torque-measuring system. The spin moment resulting from the contact of the two specimens is recorded by a strip-chart potentiometer connected to the torque-measuring system.
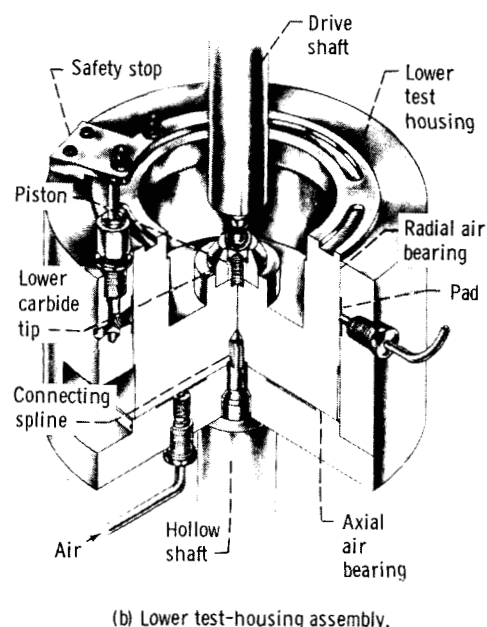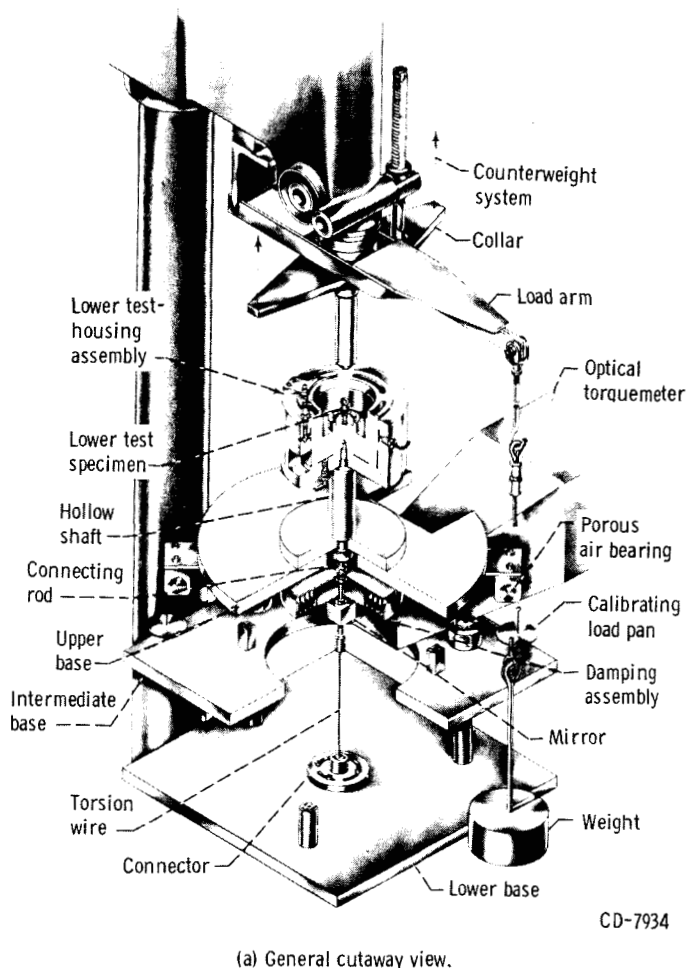
4

(a) General cutaway view.

(b) Lower test-housing assembly.

CD-7934

Figure 3. - Spinning-friction apparatus.

## Drive Assembly

The drive assembly consists of a direct-current motor, two pulleys, a drive belt, a drive shaft, and suitable supporting members (fig. 2). The direct-current drive motor is vertically mounted on a horizontal support member and has a variable speed range to 1750 rpm, which can turn the drive shaft to 3500 rpm. A drive pulley is attached to the upper end of the drive-motor shaft. The drive shaft, also vertically positioned, has the driven pulley splined to its upper end. Torque is transmitted from the drive pulley to the driven pulley by means of the drive belt. The drive shaft is supported on an upper ball bearing and a lower duplex pair of ball bearings in a shaft housing. Both ball-bearing assemblies are grease lubricated. The lower end of the drive shaft is fitted with a center-bored carbide tip that meets with the upper test specimen and drives it by means of friction. A centrally drilled hole from the carbide tip extends upwards through the drive shaft until it meets a cross-drilled hole at $90^{\circ}$ (see fig. 2). A removable vacuum

5

line (not shown) is attached to the drive shaft to hold the upper test specimen in place when the shaft is raised.

## Load Assembly

The load assembly (see fig. 2) has a hydrostatic air-lubricated journal bearing supporting the shaft housing in the horizontal support member. Inlets are provided in the hydrostatic bearing in order to accommodate pressurized air from a manifold. A collar is attached at the lower end of the shaft housing through which the load arm is positioned having a fulcrum at the collar and a pivot attached to the horizontal support member. A counterweight system is attached to the ends of the collar (fig. 3(a)) to balance the weight of the drive assembly and the attached load arm in order to more closely control the net resulting load. The air bearing assures proper alinement and provides a high stiffness support for the drive shaft, while allowing precise specimen loading. In operation, a dead weight is placed on the load arm, that loads the upper test specimen (attached to the drive shaft) against the lower test specimen.

## Lower Test Housing and Bearing Assembly

The lower test specimen is located in a lower test housing supported and centrally positioned below the drive shaft by an air-bearing assembly (see fig. 3). The air-bearing assembly consists of a radial and an axial air bearing in combination. The radial air bearing has four pads circumferentially located around the inner diameter of a vertical cylinder. The axial air bearing also has a series of four pads equally located around the center of a circular plate. The air-bearing assembly is connected to a circular upper base through a hollow shaft. The upper base is supported on three columns fastened to an intermediate base. In turn, the intermediate base is supported on the lower base by three additional support columns. The lower base is rigidly attached to the supporting structure of the apparatus.

## Torque-Measuring System

The lower test-specimen housing is prevented from rotating under the action of the spinning torque by a torsion wire (fig. 3(a)). The torsion wire is centrally positioned and fastened to the lower test-housing assembly by a connecting spline that passes through the hollow shaft described previously (fig. 3(b)). The wire is connected to the lower base by

a bolted connector. The torsion wire is removable and can be changed to accommodate different wire size diameters. A mirror, mounted on a connecting rod, turns as the torsion wire reacts to the spinning torque. Attached to the intermediate base is an optical torquemeter. Light from an incandescent bulb in the optical torquemeter shines upon the mirror through a lense system. The light reflected from the mirror passes back through the same lense system into the optical torquemeter (not shown). For a given angular deflection of the torsion wire, the angle of the reflected light will change. The light, now reflecting at a new angle, hits light-sensitive cells within the optical torquemeter, which are mechanically coupled to a two-phase balancing motor and a precision-output potentiometer.

Electrically, the cells in series opposition are connected to a servoamplifier that drives the balancing motor and positions the cells so that the gap or space between the two cells follows the final image. The output voltage, which is a linear function of cell displacement, is fed to a strip-chart potentiometer. Torque is calibrated in inch-pounds. A more detailed description of the optical torquemeter can be found in reference 8.

Since the lower test-specimen housing and torsion wire are essentially undamped, it was necessary to provide damping to reduce oscillations. A number of concentric fins attached to the lower test-specimen housing and immersed in a viscous oil (fig. 3(a)) was provided for this purpose.

The torque system is calibrated with known weights placed on two small calibrating pans. A nylon cord wound around the connecting rod is connected to the pans with Mylar straps that are supported on pressurized porous air bearings. The porous air bearings provide friction-free pivots for the straps.
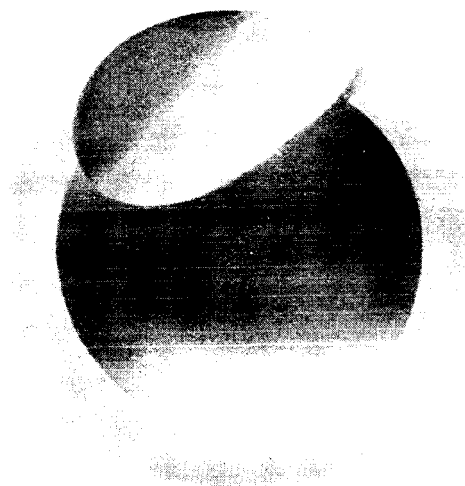
## Test Specimens

The upper test specimen is a conventional bearing ball of suitable diameter and material manufactured to different metallurgical and engineering specifications.

The lower test specimen (fig. 4(a)) is a bearing ball with a flat ground on it. Parallel to the flat, a cylindrical groove having a radius $R_1$ is ground. The radius $R_1$ can be varied from that of the upper test-specimen radius to infinity (a flat). An isometric view of the lower test specimen is shown in figure 4(b). The surface of the groove is finished to 2 microinches root mean square or better (equal to the surface finish of the upper test specimen). Prior to loading, the lower test-specimen flat rests on a spring-loaded piston contained in a second carbide tip that is centrally positioned in the lower housing assembly. After loading, the lower test specimen is held in place and centered with respect to the upper test specimen by the second carbide tip.
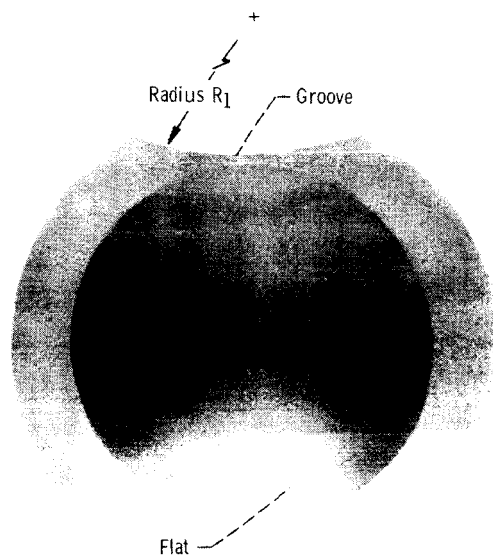
(a) Side view.

(b) Isometric view.

Figure 4. – Lower test specimen.

# OPERATING PROCEDURE

The lower test specimen is placed on the piston, and the test lubricant is put on the specimen groove. The upper test specimen is set in the tungsten-carbide tip of the drive shaft and held in place by differential pressure due to the vacuum line attached to the shaft. The drive shaft is lowered to bring the upper and lower test specimens in contact. The load arm is positioned, and a dead weight is added. The specimens can be loaded to over 400 000-psi Hertz stress. A speed is selected on the variable-speed motor. The motor is subsequently started, and the upper test specimen is driven with an angular velocity against the lower test specimen. The lubricant within the contact area is collected in a centercup of the lower test housing. The resulting spinning torque $M_s$ is recorded on the strip-chart recorder. If the torque is too high, a safety stop, integral with a slot in the lower housing assembly, prevents the assembly from rotating more than $10^o$.

The spinning-friction coefficient $f_s$ can be calculated from the following equation (refs. 5 and 9):

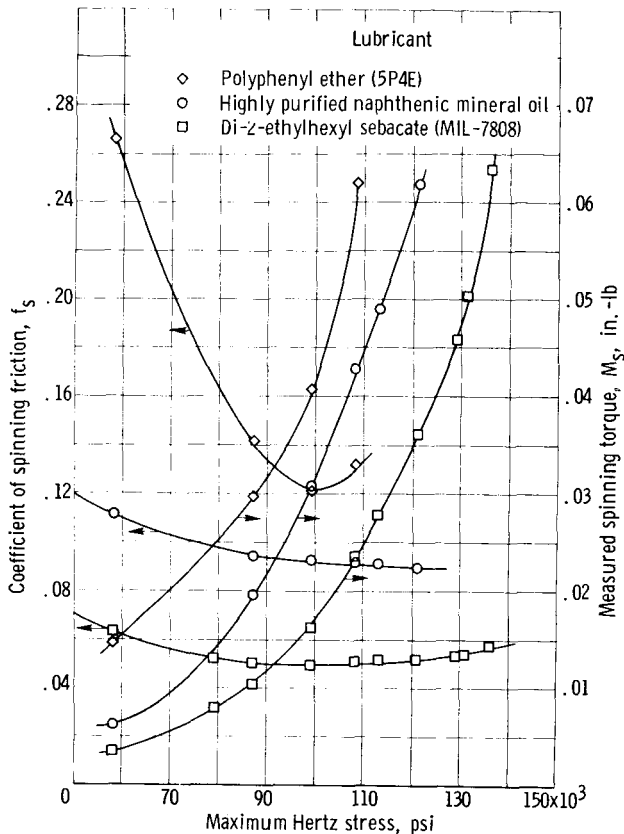$$M_s = \frac{3}{8} f_s NaE(k)$$

where

8

Figure 5. - Coefficient of spinning friction and measured spinning torque as function of maximum Hertz stress for three lubricants at spinning speed of 950 rpm with 51 percent ball-groove conformity.

## GENERAL COMMENTS

Increasing contact stress enlarges the size of the contact area. For a given shaft angular velocity, an increase in the contact stress proportionally increases the peripheral tangential speed at any point on the perimeter of the contact area of the upper test specimen. As an example, a 50 percent increase in Hertz stress results in a 50 percent increase in the tangential speed. From hydrodynamic theory, speed can affect the type of lubrication present, that is, boundary, elastohydrodynamic, or mixed. The type of lubrication present in the outer portion of the contact area may greatly affect the measured spinning torque.

It is speculated that mixed lubrication occurs in the region of decreasing coefficient of spinning friction shown in figure 5. Where the coefficient of spinning friction becomes minimum, it is probable that elastohydrodynamic lubrication prevails. At loads greater than those associated with the minimum friction values, however, the effect of contact stress on film thickness may be greater than the speed effect, and it is speculated that mixed lubrication again predominates.

Additional data must be generated with the spinning-friction apparatus to significantly sustain the speculations made and the trends shown herein.

## SUMMARY OF RESULTS

An apparatus has been designed and constructed that simulates the spinning friction in a ball-race contact to stress levels greater than 400 000-psi maximum Hertz stress, spinning speeds to 3500 rpm, and under varying contact configurations and conditions.

Preliminary tests were conducted under conditions of constant spinning speed, constraint conformity, and varying maximum Hertz stress to 136 000 psi with a polyphenyl ether (5P4E), a highly purified naphthenic mineral oil, and a di-2-ethylhexyl sebacate

| $M_s$ | measured spinning torque |
|---|---|
| $f_s$ | coefficient of spinning friction |
| N | normal load |
| a | major semiaxis of the contact ellipse |
| E(k) | complete elliptic integral of the second kind |
| k | $\left[1 - \left(\dfrac{b}{a}\right)^2\right]^{1/2}$ |
| b | minor semiaxis of the contact ellipse |

## PRELIMINARY MEASUREMENTS

Preliminary spinning-torque measurements were made under constant spinning speed, a 51 percent conformity, varying Hertz stress, and with three different types of lubricants. Test conditions were as follows:

(1) Upper test specimen: 1/2-inch-diameter SAE 52100 steel 25 grade ball; Rockwell C hardness, ~63

(2) Lower test specimen: SAE 52100 steel; Rockwell C hardness, ~63; cylindrical groove of radius $R_1$ = 0.255 inch (51 percent conformity)

(3) Normal load, N, lb: 7.0 to 59.5 producing calculated maximum Hertz stress of 58 000 to 136 000 psi, respectively

(4) Spinning velocity, $\omega_s$, rpm: 950

(5) Temperature: ambient (no heat added)

(6) Lubricants:

(a) Polyphenyl ether (5P4E): viscosity, 363 and 13.1 centistokes at $100^O$ and $210^O$ F, respectively

(b) Highly purified naphthenic mineral oil: viscosity, 79 and 8.4 centistokes at $100^O$ and $210^O$ F, respectively

(c) Di-2-ethylhexyl sebacate (MIL-7808): viscosity, 13.39 and 3.51 centistokes at $100^O$ and $210^O$ F, respectively

The measured spinning torque $M_s$ and the resulting calculated coefficients of spinning friction for these tests are shown in figure 5. As the maximum Hertz stress increases, the coefficient of spinning friction decreases to a minimum value for the three lubricants tested. This trend is shown in reference 5 for the same stress levels with a MIL-7808 lubricant. For a constant spinning speed and ball-groove conformity, spinning friction appears to be a function of lubricant and contact stress.

(MIL-7808) as lubricants. It was found that the calculated coefficient of spinning friction decreased with increasing stress to an intermediate stress level for the three lubricants tested. The minimum coefficients of spinning friction were 0.122, 0.089, and 0.050 for each lubricant, respectively.

Lewis Research Center,
   National Aeronautics and Space Administration,
      Cleveland, Ohio, February 11, 1965.

# REFERENCES

1. Bisson, Edmond E.; and Anderson, William J.: Advanced Bearing Technology. NASA SP-38, 1964.

2. Jones, A. B.: Ball Motion and Sliding Friction in Ball Bearings. J. Basic Eng. (ASME Trans.), ser. D, vol. 81, no. 1, Mar. 1959, pp. 1-12.

3. Johnson, K. L.: Tangential Tractions and Micro-Slip in Rolling Contact; Rolling Contact Phenomena, J. B. Bidwell, ed., Elsevier Pub. Co., 1962, pp. 6-28.

4. Johnson, K. L.: A Note on the Influence of Elastic Compliance on Sliding Friction in Ball Bearings. J. Basic Eng. (ASME Trans.), ser. D, vol. 82, no. 4, Dec. 1960, pp. 889-890.

5. Reichenbach, G. S.: The Importance of Spinning Friction in Thrust-Carrying Ball Bearings. J. Basic Eng. (ASME Trans.), ser. D, vol. 82, no. 2, June 1960, pp. 295-301.

6. Jones, A. B.: A General Theory for Elastically Constrained Ball and Radial Roller Bearings Under Arbitrary Load and Speed Conditions. J. Basic Eng. (ASME Trans.), ser. D, vol. 82, no. 2, June 1960, pp. 309-320.

7. Mindlin, R. D.: Compliance of Elastic Bodies in Contact. J. Appl. Mech., vol. 16, no. 3, Sept. 1949, pp. 259-268.

8. Krsek, Alois, Jr.; and Tiefermann, Marvin (With appendix by Donald R. Buchele): Optical Torquemeter for High Rotational Speeds. NASA TN D-1437, 1962.

9. Poritsky, H.; Hewlett, C. W., Jr.; and Coleman, R. E., Jr.: Sliding Friction of Ball Bearings of the Pivot Type. J. Appl. Mech., vol. 14, no. 4, Dec. 1947, pp. 261-268.